Decentralized Approach for Fault Diagnosis of Three Cell Converters

Hanane Louajri, Moamar Sayed-Mouchaweh

Université Lille Nord de France, Mines-Douai, IA 941, rue Charles Bourseul 59508 Douai, France

(e-mail: [hanane.louajri, moamar.sayed-mouchaweh]@mines-douai.fr).

ABSTRACT

In this paper, an approach for fault diagnosis of hybrid dynamic systems (HDS), in particular discretely controlled continuous system, is proposed. The goal is to construct a decentralized diagnosis structure, able to diagnose parametric and discrete faults. This approach considers the system as composed of a set of interacted hybrid components (HCs). Each HC is composed of a discrete component (Dc), e.g. on/off switches, with the continuous components (Ccs), e.g. capacitors, whose continuous dynamic behavior is influenced by the Dc discrete states. A local hybrid diagnosis module, called diagnoser, is associated to each HC in order to diagnose the faults occurring in this HC. In order to take into account the interactions between the different HCs, local diagnosis decisions are merged using a coordinator. The latter issues a final decision about the origin of the fault and identifies its parameters. The advantage of the proposed approach is that local hybrid diagnosers as well as the coordinator are built using local models. The proposed approach is applied to achieve the decentralized diagnosis of discrete and parametric faults of power electronic three-cell converters.

1. INTRODUCTION

1.1 Basic definitions and motivation

A fault can be defined as a non-permitted deviation of at least one characteristic property of a system or one of its components from its normal or intended behavior. Fault diagnosis is the operation of detecting faults and determining possible candidates that explain their occurrence. Most of real systems are hybrid dynamic systems (HDS) (Zaytoon, 2001), (Arogeti *et al.*, 2010) in which the discrete and continuous dynamics cohabit. Therefore, fault diagnosis of HDS must deal with the evolution of continuous dynamics in each discrete mode in

order to construct a diagnosis module (called diagnoser) able to diagnose parametric and discrete faults. Parametric faults affect the system continuous dynamics and are characterized by abnormal changes in some system parameters; whereas discrete faults affect the system discrete dynamics and are considered either as the occurrence of unobservable events and/or reaching discrete fault modes. In both cases, they entail unpredicted, abnormal, change in the system configuration. Therefore faults may be modelled in HDS by introducing parameters into the system model, explicit fault events or/and fault modes.

Discretely controlled continuous systems (DCCS) (Schild and Lunze, 2008) are a special class of HDS widely used in the literature. In these systems, the changes in discrete modes are achieved by discrete control commands, e.g. opening or closing a switch.

1.2 State of the art

Many approaches have been proposed in the literature for fault diagnosis of DCCS. They are generally divided into three main categories:

- approaches for the diagnosis of parametric faults,

- approaches for the diagnosis of discrete faults,

- approaches for the diagnosis of both parametric and discrete faults.

In parametric fault diagnosis approaches, (Cocquempot *et al.*, 2004), (Alavi *et al.*, 2011), (Kamel *et al.*, 2012) relations over observable variables are computed in order to generate residuals sensitive to a certain subset of parametric faults in each observable discrete mode.

The discrete fault diagnosis approaches are divided into three main groups. In the first group (Rahiminejad *et al.,* 2012), (Defoort *et al.*, 2011), residuals sensitive to the continuous dynamics in each discrete mode are defined. If unpredicted change occurs due to the occurrence of unobservable discrete fault, the residuals, defined for the

discrete mode before the fault occurrence, will be different of zero in the discrete mode after the fault occurrence. This change of residuals values from zero indicates the occurrence of a discrete fault. The approaches of second group (Bhowal *et al.*, 2007), (Biswas *et al.*, 2006), describe in each normal or fault discrete mode, continuous dynamics as the rate of changes of continuous variables. These rates are considered to be constant. Transition guards are defined as linear inequalities based on continuous variables values. When a guard is satisfied, its corresponding mode transition is enabled. The occurrence of a fault is diagnosed by determining the discrete state reached due to specific guard satisfaction. In the methods of last group (Bayoudh *et al.*, 2006), a set of residuals is defined in each normal or fault discrete mode. Each residual is characterized by three symbols: 0, 1 or *und* when the residual value is, respectively, zero, different of zero and undefined. *und* represents the case where the associated residual is not defined in the new active mode. These symbols are used to distinguish the different normal and fault discrete modes. A discrete fault is isolated by determining the current discrete fault mode of the system.

The third category includes few approaches for the diagnosis of both parametric and discrete faults. Some approaches of this category (Derbel *et al.*, 2009), capture the continuous dynamics by integrating the occurrence time of events. They consider that the occurrence of discrete or parametric faults does not change events ordering but only alters their timing characteristics. Therefore, a discrete or parametric fault is diagnosed when predicted events occur too late or too early or they do not occur at all during their predefined time intervals. Other methods (Daigle *et al.*, 2010), construct temporal causal graphs (TCG) for each normal and fault discrete mode based on the use of a global hybrid bond graph. When measurement deviations, caused by fault occurrence, are observed through residuals, TCG are used to determine the effects that faults will have on the measurements as well as the temporal order in which they deviate. Then, fault signature is defined for each fault as the qualitative value of the magnitude and the first non-zero derivative change which can be observed in the residuals. In order to distinguish parametric from discrete faults, the signatures are extended by adding discrete symbols indicating abrupt changes from zero to non-zero or from non-zero to zero. In (Louajri *et al.*, 2013), an approach based on a diagnoser with hybrid structure is developed. It consists of three parts: the discrete diagnoser, the continuous diagnoser and the coordinator. The discrete diagnoser is built using a discrete time hybrid automata representing global model. It exploits the information extracted from the system continuous dynamics to get rid of diagnosis ambiguity due to the system behavior abstraction. The continuous diagnoser generates residuals. The latter compare the measured and nominal values of each continuous variable in order to diagnose the parametric

faults in each discrete mode. The information about the discrete mode is provided to the continuous diagnoser thanks to the information extracted from the discrete dynamics. Finally, the coordinator uses the decisions issued from the discrete and continuous diagnosers in order to diagnose faults requiring the interaction between both diagnosers.

1.3 Our approach

Fault diagnosis approaches of the literature do not scale to HDS with a large number of discrete modes because they achieve fault diagnosis using one centralized diagnosis module. The latter is built using a global model of the system. Two problems are arisen -) the weak robustness in the sense that, when the global diagnosis module fails, this may bring down the entire diagnosis task and -) the system global model can be too huge to be physically constructed. Therefore in this paper, the proposed approach of (Louajri *et al.*, 2013) is developed to achieve the diagnosis of parametric and discrete faults in decentralized manner using several local hybrid diagnosers. The latter are constructed without the use of a global model of the system but only the local models of the system discrete components (Figure 1).

The paper is organized as follows. In section 2, the three cell converter system is described and modelled. Section 3 defines the steps of the hybrid diagnosis construction. In section 4, a simulation for the three-cell converter is used to demonstrate the efficacy of the approach. A conclusion with the future work ends the paper in section 5.
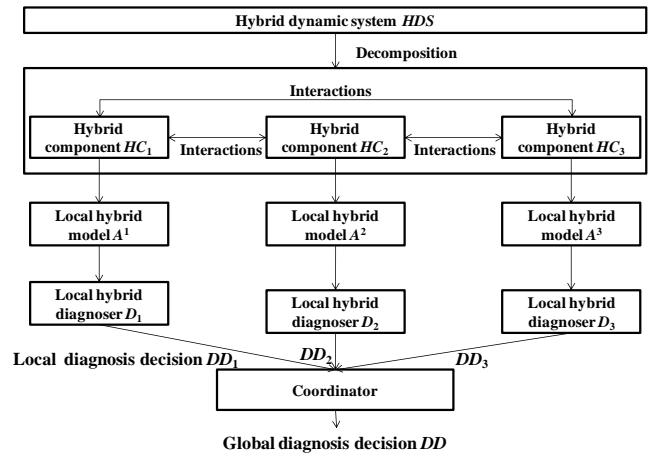

Figure 1. Decentralized hybrid diagnosis structure for a HDS composed of 3 interacted HCs.

2. THREE CELL CONVERTER DESCRIPTION AND MODELING

2.1. System description

In order to illustrate the proposed approach, the decentralized fault diagnosis of three-cell converters

(Shahbazi *et al*., 2013) (Trigeassou, 2011), depicted in Fig.2, is achieved. With the same observability used in the literature (Defoort *et al*., 2011), (Uzunova *et al*., 2012) for the three-cell converter diagnosis, the proposed approach has the advantage to diagnose (not only detect) discrete and parametric faults using a decentralized structure.

The continuous dynamics of the system are described by state vector $X = [Vc_1 \quad Vc_2 \quad I]^T$, where Vc_1 and Vc_2 represent, respectively, the floating voltage of capacitors C_1 and C_2 and I represents the current flowing from source E towards load (R,L) through three elementary switching cells $S_j, j \in \{1,2,3\}$. The latter represent the system discrete dynamics. Each discrete switch S_j has two discrete states: S_j opened ($h_q^j = 0$) or S_j closed ($h_q^j = 1$), where h_q^j is the state discrete output of S_j. The control of this system has two main tasks: -) balancing the voltages between the switches and -) regulating the load current to a desired value. To accomplish that, the controller changes the switches' states from opened to closed or from closed to opened by applying discrete commands 'close' or 'open' to each discrete switch $S_j, j \in \{1,2,3\}$ (see Fig.2). Thus, the considered example is a DCCS.
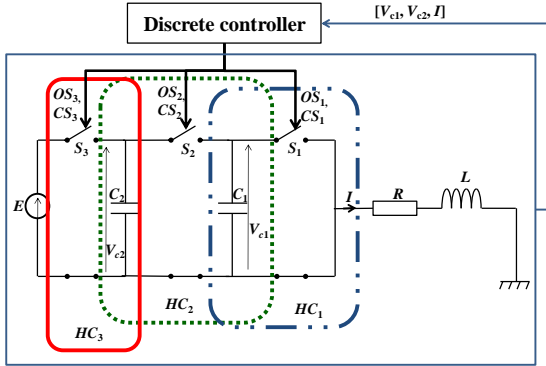

Figure 2. Three-cell converter discription and decomposition

2.2. System modeling and decomposition

The real system dynamic evolution of three-cell converter is written as (Defoort *et al*., 2011)

$$
\begin{cases}
\dot{V}c_1 = -h_q^1 \frac{1}{C_1} I + h_q^2 \frac{1}{C_1} I \\
\dot{V}c_2 = -h_q^2 \frac{1}{C_2} I + h_q^3 \frac{1}{C_2} I \\
\dot{I} = -\frac{R}{L} I + h_q^1 \frac{1}{L} Vc_1 + h_q^2 \frac{1}{L} (Vc_2 - Vc_1) + h_q^3 \frac{1}{L} (E - Vc_2)
\end{cases}
\tag{1}
$$

As shown in (1), the discrete state of S_1, represented by a real discrete output h_q^1, influences the dynamic evolution of Vc_1 and I. The discrete state of S_2, represented by h_q^2, impacts the dynamic evolution of Vc_1, Vc_2 and I. The discrete state of S_3, represented by h_q^3, influences the dynamic evolution of Vc_1 and Vc_2. Thus, the three-cell

converter system is decomposed into three interacted HCs as shown in Fig.2:

- HC_1 is composed of switch S_1 $(Dc_1), Vc_1$ (Cc_1) and I (Cc_3).

- HC_2 is composed of switch S_2 (Dc_2), Vc_1 (Cc_1), Vc_2 (Cc_2) and I (Cc_3).

- HC_3 is composed of switch S_3 $(Dc_3), Vc_2$ (Cc_2) and I (Cc_3).

In the literature (Defoort *et al*., 2011), (Uzunova *et al*., 2012), eight faults are considered for the diagnosis of the three-cell converters system (Table 1).

Table 1. Faults for the diagnosis of three-cell converters

Fault types	*Fault labels*	*Fault description*
Discrete faults	F_1	S_1 stuck opened
	F_2	S_1 stuck closed
	F_3	S_2 stuck opened
	F_4	S_2 stuck closed
	F_5	S_3 stuck opened
	F_6	S_3 stuck closed
Parametric faults	F_7	Change in the nominal parameter values of C_1 due to C_1 ageing
	F_8	change in the nominal parameter values of C_2 due to C_2 ageing

Labels N_1, N_2 and N_3 signify the normal operating modes for, respectively, HC_1, HC_2 and HC_3.

2.3. Residuals generation

In order to show the influence of each discrete component on the dynamic evolution of each continuous component, (1) is rewritten as follows:

$$
\begin{cases}
\dot{V}c_1 = \dot{V}c_1^1 + \dot{V}c_1^2 \\
\dot{V}c_2 = \dot{V}c_2^2 + \dot{V}c_2^3 \\
\dot{I} = \dot{I}_c + \dot{I}^1 + \dot{I}^2 + \dot{I}^3
\end{cases}
\tag{2}
$$

where $\dot{V}c_1^1 = -h_q^1 \frac{1}{C_1} I$, $\dot{V}c_1^2 = h_q^2 \frac{1}{C_1} I$, $\dot{V}c_2^2 = -h_q^2 \frac{1}{C_2} I$, $\dot{V}c_2^3 = h_q^3 \frac{1}{C_2} I$, $\dot{I}_c = -\frac{R}{L} I$, $\dot{I}^1 = h_q^1 \frac{1}{L} Vc_1$, $\dot{I}^2 = h_q^2 \frac{1}{L} (Vc_2 - Vc_1)$, $\dot{I}^3 = h_q^3 \frac{1}{L} (E - Vc_2)$.

$\dot{V}c_1^1$ represents the real dynamic evolution of Vc_1 according to the discrete state of S_1 (Dc_1). Likewise, $\dot{V}c_1^2$, $\dot{V}c_2^2$, $\dot{V}c_2^3$, $\dot{I}^1$, $\dot{I}^2$ and $\dot{I}^3$ have the same definition as $\dot{V}c_1^1$. $\dot{I}_c$ represents the part of dynamic evolution of I which does not depend on the discrete state of any switch.

Similarly, considering that the parametric faults related to the load (R, L) are not considered, the equations system for the nominal dynamic evolution of system components can be written as:

3

$$\begin{cases} \tilde{V}c_1 = \tilde{V}c_1^1 + \tilde{V}c_1^2 \\ \tilde{V}c_2 = \tilde{V}c_2^2 + \tilde{V}c_2^3 \\ \tilde{I} = \tilde{I}_c + \tilde{I}^1 + \tilde{I}^2 + \tilde{I}^3 \end{cases} \quad (3)$$

$\tilde{V}c_1^1 = -\tilde{h}_q^1 \frac{1}{\tilde{C}_1} I, \quad \tilde{V}c_1^2 = \tilde{h}_q^2 \frac{1}{\tilde{C}_1} I, \quad \tilde{V}c_2^2 = -\tilde{h}_q^2 \frac{1}{\tilde{C}_2} I, \quad \tilde{V}c_2^3 = \tilde{h}_q^3 \frac{1}{\tilde{C}_2} I, \tilde{I}_c = \dot{I}_c = -\frac{R}{L} I \quad \tilde{I}^1 = \tilde{h}_q^1 \frac{1}{L} Vc_1, \quad \tilde{I}^2 = \tilde{h}_q^2 \frac{1}{L} (Vc_2 - Vc_1), \quad \tilde{I}^3 = \tilde{h}_q^3 \frac{1}{L} (E - Vc_2)$ where $\tilde{h}_q^1$, $\tilde{h}_q^2$ and $\tilde{h}_q^3$ are the nominal values of states q_1, q_2 and q_3 discrete outputs while $\tilde{C}_1$ and $\tilde{C}_2$ are the nominal values of C_1 and C_2. Based on (2) and (3), residuals r_1, r_2 and r_3 are generated as follows:

$$\begin{cases} r_1 = \left(-\tilde{h}_q^1 \frac{1}{\tilde{C}_1} + h_q^1 \frac{1}{C_1}\right) I + \left(\tilde{h}_q^2 \frac{1}{\tilde{C}_1} - h_q^2 \frac{1}{C_1}\right) I \\ r_2 = \left(-\tilde{h}_q^2 \frac{1}{\tilde{C}_2} + h_q^2 \frac{1}{C_2}\right) I + \left(\tilde{h}_q^3 \frac{1}{\tilde{C}_2} - h_q^3 \frac{1}{C_2}\right) I \\ r_3 = \left(\tilde{h}_q^1 - h_q^1\right) \frac{Vc_1}{L} + \left(\tilde{h}_q^2 - h_q^2\right) \frac{(Vc_2 - Vc_1)}{L} \\ \quad + \left(\tilde{h}_q^3 - h_q^3\right) \frac{(E - Vc_2)}{L} \end{cases} \quad (4)$$

In order to show the influence of each discrete component on the residuals, (4) is rewritten as follows:

$$\begin{cases} r_1 = r_1^1 + r_1^2 \\ r_2 = r_2^2 + r_2^3 \\ r_3 = r_{3c} + r_3^1 + r_3^2 + r_3^3 \end{cases} \quad (5)$$

where $r_1^1 = \left(-\tilde{h}_q^1 \frac{1}{\tilde{C}_1} + h_q^1 \frac{1}{C_1}\right) I = \left(\tilde{V}c_1^1 - \dot{V}c_1^1\right)$, $r_1^2 = \left(\tilde{V}c_1^2 - \dot{V}c_1^2\right)$, $r_2^2 = \left(\tilde{V}c_2^2 - \dot{V}c_2^2\right)$, $r_2^3 = \left(\tilde{V}c_2^3 - \dot{V}c_2^3\right)$, $r_3^1 = \left(\tilde{I}^1 - \dot{I}^1\right)$, $r_3^2 = \left(\tilde{I}^2 - \dot{I}^2\right)$, $r_3^3 = \left(\tilde{I}^3 - \dot{I}^3\right)$ and $r_{3c} = \left(\tilde{I}_c - \dot{I}_c\right) = 0$.

2.4. Hybrid automata construction

Hybrid automata A^1 characterizing the hybrid dynamics of HC_1 is defined by the tuple (see Fig.4 and Fig.4):

$$A^1 = (Q^1, \Sigma^1, SP^1, \delta^1, X^1, flux^1, r^1, Init^1) \quad (6)$$

where,

$Q^1 = \{S_1 O$ (S_1 opened), $S_1 C$ (S_1 closed), $S_1 SO$ (S_1 stuck opened), $S_1 SC$ (S_1 stuck closed)$\}$: is a finite set of discrete states (discrete modes) of S_1. The output of state q_k^1 is characterized by real discrete output vector $h_q^1 \in \{0$ (when S_1 is opened), 1 (when S_1 is closed)$\}$ and nominal discrete output vector $\tilde{h}_q^1 = \{0$ (when S_1 have to be opened), 1 (when S_1 have to be closed)$\}$. At normal discrete mode (state) $\tilde{h}_q^1 = h_q^1$ while in faulty mode $\tilde{h}_q^1 \neq h_q^1$;

$\Sigma^1 = \Sigma_o^1 \cup \Sigma_u^1$ is the event set of S_1. It includes observable events corresponding to control command events $\Sigma_o^1 = \{CS_1$ (close S_1), OS_1 (open S_1)$\}$ and unobservable events Σ_u^1 including fault events. $\Sigma_f^1 = \{S_1\_stuck\_open,$

$S_1\_stuck\_close$, $f_{\tilde{C}_1 \neq C_1}\}$ denotes the set of fault events (discrete and parametric) that can occur in HC_1. The set of fault events contains three different fault types or modes indicated by the fault labels: $\{F_1, F_2, F_7\}$. The set of labels for HC_1 is $SP^1 = \{N_1, F_1, F_2, F_7\}$.

$\delta^1: Q^1 \times \Sigma^1 \rightarrow Q^1$: is the state transition function. A transition $\delta^1(q^1, e) = q^{1+}$ corresponds to a change from state q^1 to state q^{1+} after the occurrence of event $e \in \Sigma^1$;

$X^1 = \{Vc_1, Vc_2, I\}$ is a finite set of continuous variables associated to S_1;

$flux^1: Q^1 \times X^1 \rightarrow \mathbb{R}^n = \{\tilde{X}^1, \dot{X}^1\}$: is a function characterizing temporal evolution $\dot{X}^1$ and nominal evolution $\tilde{X}^1$ of continuous variables X^1 in each discrete state q_k^1, where $\tilde{X}^1 = [\tilde{V}c_1^1 \quad \tilde{V}c_2^1 \quad \tilde{I}^1]^T$, $\dot{X}^1 = [\dot{V}c_1^1 \quad \dot{V}c_2^1 \quad \dot{I}^1]^T$;

$Init^1 \subset Q^1 \times X^1 = S_1 O (q_0^1)$: is the set of initial conditions.
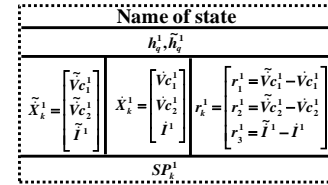

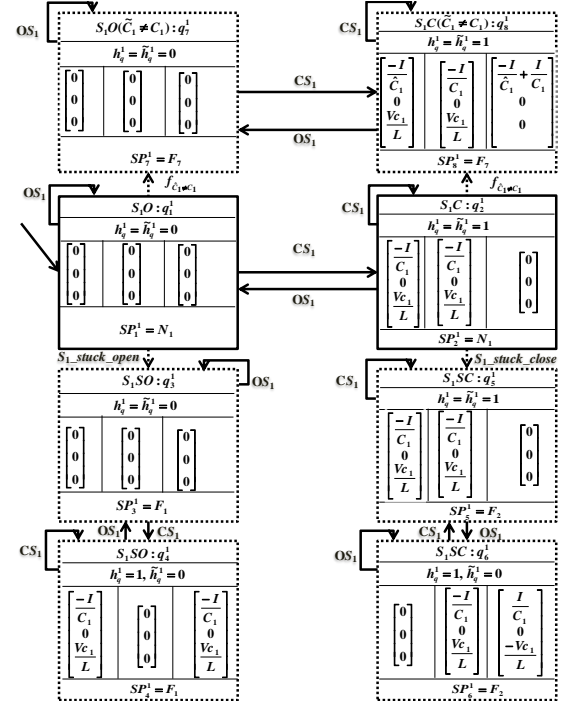Figure 3. Hybrid state of A^1 for HC_1.

Figure 4. Hybrid automata A^1 for HC_1.

$r^1 = \{r_1^1, r_2^1, r_3^1\}$: is a set of residuals associated to HC_1;

Since Vc_2 does not belong to HC_1, therefore, $\tilde{V}c_2^1 = 0$,

$\dot{V}c_2^1 = 0$. Thus r_2^1 is equal to zero.

Hybrid automata A^2 and A^3 for HC_2 and HC_3 are constructed by the same manner.

2.5. Motivation to use the considered residuals

Let us consider the occurrence of a fault of type F_5, e.g. S_3 stuck opened. When the controller sends control command $'CS_3'$(close S_3), S_3 remains in its stuck-opened mode ($\tilde{h}_q^3 = 1$ and $h_q^3 = 0$). The occurrence of a fault of type F_5 impacts at the same time r_2 and r_3 ($\tilde{h}_q^3 = 1$ and $h_q^3 = 0$) while it does not impact r_1 (($\tilde{h}_q^1 = h_q^1$), ($\tilde{h}_q^2 = h_q^2$) and ($\tilde{C}_1 = C_1$)), see (4). Therefore, there is no delay of the influence of the fault occurrence on the sensitive residuals, e.g. r_2 and r_3. Moreover, there is no fault propagation from one residual to another one, from r_2 or r_3 towards r_1.

3. THREE CELL CONVERTER DIAGNOSIS

3.1. Global fault signature construction

A qualitative signature is constructed by generating continuous and discrete symbols from residual values. Continuous symbols $CS(r_i) \in \{0, -, +\}$ represent the qualitative abstraction of residual values into stable/increasing/decreasing ones:

- r_i^0: $r_i(t)$ belongs to the nominal interval;

- r_i^-: $r_i(t)$ is below the nominal interval;

- r_i^+: $r_i(t)$ is above the nominal interval.

The occurrence of a discrete fault exhibits an abrupt change in the continuous dynamics due to unpredicted change in Dc_j discrete mode. This change is characterized by the absence ($h_q^j = 0$ while $\tilde{h}_q^j = 1$) or the addition ($h_q^j = 1$ while $\tilde{h}_q^j = 0$) of associated term e.g., $\frac{I}{C_1}$. On the other hand, parametric faults due to the ageing effect cannot cause this abrupt change with a finite change in magnitude. In fact, they are indicated by a progressive abnormal change of the parameter value. In order to take into account this discriminative information, discrete symbols $DS(r_i)$ are added for the abstraction of each residual r_i in order to distinguish between parametric and discrete faults as follows:

- $PC_i^j = +Val$: denotes an abrupt positive change in residual r_i due to a discrete fault caused by Dc_j. $+Val$ is equal to the absolute value of the term associated to h_q^j;

- $NC_i^j = -Val$: denotes an abrupt negative change in residual r_i due to a discrete fault caused by Dc_j;

- UC_i: denotes that there is no observed abrupt change in residual r_i.

- A fault signature Sig_q at global discrete state q is the combination of continuous and discrete symbols of the different residuals as follows:

$$Sig_q = \left(r_1^{CS(r_1)}, DS(r_1)\right) \& \dots \& \left(r_n^{CS(r_n)}, DS(r_n)\right) \quad (7)$$

3.2. Local fault signature construction

Each discrete state q_k^j of A^j generates a fault signature sig_k^j as a guard over residuals r^j calculated in this discrete state as follows:

$$sig_k^j = \left(r_1^{j\,CS(r_1^j)}, DS(r_1^j)\right) \& \dots \& \left(r_n^{j\,CS(r_n^j)}, DS(r_n^j)\right) \quad (8)$$

Based on (5), we can write:

$$r_i = \tilde{x}_i - \dot{x}_i = (\tilde{x}_i^1 - \dot{x}_i^1) + \dots + (\tilde{x}_i^l - \dot{x}_i^l) = r_i^1 + \dots + r_i^l$$

If $\left[(\tilde{x}_i^j - \dot{x}_i^j) = r_i^j\right] \neq 0$, it means that the other parts of residual r_i are equal to zero (one fault can be occurred at the same time). In this case, $r_i = r_i^j$. Hence, r_i will have the continuous and discrete symbols of r_i^j. Thus (8) is rewritten as follows:

$$sig_k^j = \left(r_1^{CS(r_1)}, DS(r_1)\right) \& \dots \& \left(r_n^{CS(r_n)}, DS(r_n)\right) \quad (9)$$

By comparing (8) and (9), we can notice that sig_k^j becomes equivalent to the global fault signature Sig_q.

3.3. Local hybrid diagnoser

The objective of local hybrid diagnoser D_j is to detect and isolate the occurrence of parametric and discrete faults affecting the dynamics of hybrid component HC_j. D_j is built based on the local model, A^j, of HC_j. Each state of D_j, denoted z_k^j, is of the form shown in Fig.5.

Figure 5. State of local hybrid diagnoser D_j of HC_j.

Local hybrid diagnoser D_1 of HC_1 is depicted in Fig.6. It is constructed from hybrid automata A^1 of Fig.4.

D_1 is constructed as follows:

- Initial state z_1^1, characterized by $(Q_1^1, \tilde{X}^1, SP^1)$, is composed of the following A^1 states: q_1^1 (A^1 initial state), q_3^1 reached from q_1^1 by the occurrence of a fault event '$S_1\_stuck\_open$' (fault of type F_1) and q_7^1 reached from q_1^1 due to the occurrence of a fault event '$f_{\tilde{C}_1 \neq C_1}$' (fault of type F_7). Thus, Q_1^1 is equal to $\{q_1^1, q_3^1, q_7^1\}$. SP^1 gathers the normal and fault labels associated to the states belonging to Q_1^1. Therefore, SP^1 is equal to $\{N_1, F_1, F_7\}$.

Finally, $\tilde{X}^1$ gathers $\tilde{X}_k^1$ of all the states q_k^1 of Q_1^1. Since states q_3^1 and q_7^1 are reached from q_1^1 due to the occurrence of unobservable event (a fault), $\tilde{X}_1^1$, $\tilde{X}_3^1$ and $\tilde{X}_7^1$ are equivalent and equal to $[0 \quad 0 \quad 0]^T$ (see Fig.4).

• The states of D_1 reached due to the occurrence of each control command event observed by HC_1 are computed. Since D_1 initial state is S_1O, control command OS_1 will not change D_1 state z_1^1. The event CS_1 transits D_1 from z_1^1 to z_2^1, characterized by $(Q_2^1, \tilde{X}^1, SP^1)$. Q_2^1 is equal to all the states reached from Q_1^1 due to the occurrence of CS_1. Thus, Q_2^1 is equal to $\{q_2^1, q_4^1, q_8^1\}$ (see Fig.4). Moreover, all the states of A^1 reached from Q_2^1 due to the occurrence of unobservable event are added to Q_2^1. Therefore, Q_2^1 is equal to $\{q_2^1, q_4^1, q_8^1, q_5^1\}$. SP^1 is equal to $\{N_1, F_1, F_7, F_2\}$ while $\hat{X}^1$ is equal to $\left[\frac{-I}{C_1} \quad 0 \quad \frac{Vc_1}{L}\right]^T$ (see Fig.4).

• Fault signatures are generated for each D_1 state thanks to the continuous dynamic evolution in each discrete state of Q_k^1. In the initial D_1 state, z_1^1, the continuous dynamic evolution in any state of Q_1^1 does not evolve. Therefore, their associated residuals are equal to zero leading to obtain the fault signature Sig_N^1 (see Table 2). In z_2^1, the continuous dynamic evolution of the states belonging to Q_2^1 will allow to generate four fault signatures as we can see in Fig.6. They allow to detect and isolate discrete and parametric faults F_1 and F_7 as follows. q_4^1 of A^1 (reached due to the occurrence of fault of type F_1) generates local fault signature $Sig_{q_4^1}^1$.

$Sig_{q_4^1}^1 = \left(r_1^{1-}, \frac{-I}{C_1}\right) \& (r_2^{10}, UC_2) \& \left(r_3^{1+}, \frac{Vc_1}{L}\right)$ (see the values of local residuals in q_4^1 of Fig.4). As explained in subsection 3.2, local fault signature $Sig_{q_4^1}^1$ is equal to global fault signature.

$$Sig_q = \left(r_1^{CS(r_1)}, DS(r_1)\right) \& \left(r_2^{CS(r_2)}, DS(r_2)\right) \&$$

$$\left(r_3^{CS(r_3)}, DS(r_3)\right) = \left(r_1^-, \frac{-I}{C_1}\right) \& (r_2^0, UC_2) \& \left(r_3^+, \frac{Vc_1}{L}\right).$$

This global signature is used as transition to isolate the occurrence of a fault of type F_1. Same reasoning can be applied for the other fault signatures. To overcome the noise problem, the values of comparison (e.g., $\frac{I}{C_2}$) are replaced by the intervals corresponding to the selected confidence level. These intervals are calculated using Z-test in order to determine the thresholds of each value.

Same reasoning can be followed for the construction of the other states of D_1.

It is worth pointing out that $Sig_q = Sig_{q_4^1}^1 = \left(r_1^-, \frac{-I}{C_1}\right) \& (r_2^0, UC_2) \& \left(r_3^+, \frac{Vc_1}{L}\right)$ means that the three conditions have to be satisfied in order to enable
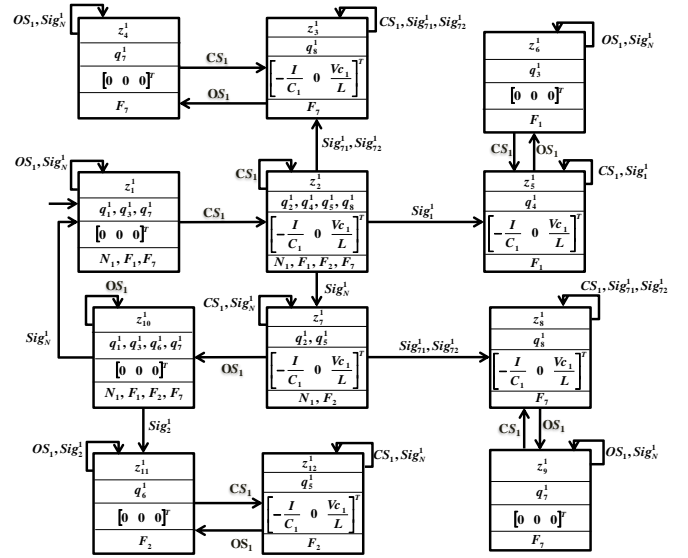
the corresponding transition.

Figure 6. Local hybrid diagnoser D_1 of HC_1.

Table II shows the local fault signatures (equivalent to the global fault signatures) used by D_1 to achieve its local diagnosis.

Table 2. Local fault signatures generated due to the occurrence of faults in HC_1.

SP^1	Local signature name	Equivalent global fault signatures
F_1	Sig_1^1	$\left(r_1^-, \frac{-I}{C_1}\right) \& (r_2^0, UC_2) \& \left(r_3^+, \frac{Vc_1}{L}\right)$
F_2	Sig_2^1	$\left(r_1^+, \frac{I}{C_1}\right) \& (r_2^0, UC_2) \& \left(r_3^-, \frac{-Vc_1}{L}\right)$
F_7	Sig_{71}^1	$(r_1^-, UC_1) \& (r_2^0, UC_2) \& (r_3^0, UC_3)$
	Sig_{72}^1	$(r_1^+, UC_1) \& (r_2^0, UC_2) \& (r_3^0, UC_3)$
N_1	Sig_N^1	$(r_1^0, UC_1) \& (r_2^0, UC_2) \& (r_3^0, UC_3)$

The other diagnosers D_2 and D_3 for HC_2 and HC_3 can be constructed similarly as for D_1. D_2 is sensitive to discrete faults F_3 and F_4 and to parametric faults F_7 and F_8, while D_3 is sensitive to discrete faults F_5 and F_6 and to parametric fault F_8. The occurrence of parametric fault F_7 (respectively F_8) is detected intrinsically by D_1 and D_2 (respectively D_2 and D_3).

3.4. Coordinator construction

The system decomposition achieved by the proposed approach allows each local hybrid diagnoser to diagnose faults that can occur in its corresponding hybrid component. In order to obtain a decentralized diagnosis performance equivalent to a centralized diagnoser, a decision coordinator is defined. It generates a global diagnosis decision by merging local diagnosis decisions provided by local hybrid diagnosers. Let us denoted F^1, F^2 and F^3 the faults that can

occur, respectively, in HC_1, HC_2 and HC_3. $F^1 \in \{F_1, F_2, F_7\}$, $F^2 \in \{F_3, F_4, F_7, F_8\}$ and $F^3 \in \{F_5, F_6, F_8\}$,. Global diagnosis decision DD is computed as follows:

- D_1 diagnoses with certainty the occurrence of a fault of type F^1 through the global fault signature Sig_q. D_2 cannot diagnose with certainty the occurrence of this fault because it does not belong to its associated HC_2. D_3 cannot diagnose with certainty the occurrence of this fault because it does not belong to its associated HC_3. Therefore, the global diagnosis decision will be $DD = F^1$.

- Global fault signature Sig_q corresponds to a fault of type F^1 or of type F^2 (F_7). Thus, global diagnoser DD will be F^1 or F^2. Both D_1 and D_2 are sensitive to this fault signature, therefore D_1 declares F_7; and D_2 declares F_7. In order to obtain a decentralized diagnosis decision equivalent to the global one, global diagnosis decision DD will be equal to $(F^1 \text{ or } F^2) = F_7$.

- Table 3 shows global diagnosis decision DD. A local diagnoser declares 'nothing' when it cannot confirm the occurrence or the non-occurrence of a fault.

Table 3. Global diagnosis decision DD for Three Cell Converter .

cases	Local diagnoser D_1	Local diagnoser D_2	Local diagnoser D_3	Global decision DD
1	N_1	N_2	N_3	N
2	F^1	N_2 or Nothing	N_2 or Nothing	F^1
3	N_1 or Nothing	F^2	N_3 or Nothing	F^2
4	F^1	F^2	N_3 or Nothing	F^1 or F^2
5	N_1 or Nothing	F^2	F^3	F^2 or F^3
6	N_1 or Nothing	N_2 or Nothing	F^3	F^3
7	Nothing	Nothing	Nothing	Nothing

3.5. Identification of parametric faults

When one of parametric faults is diagnosed, its real value needs to be identified. As an example, for parametric fault of type F_7 related to C_1, the real value of the latter is identified based on its corresponding residual as follows:

$$r_1 = \left(-\frac{1}{\tilde{C}_1} + \frac{1}{C_1}\right) \Rightarrow C_1 = \frac{\tilde{C}_1}{\tilde{C}_1 r_1 + 1} \qquad (10)$$

$$r_2 = \left(+\frac{1}{\tilde{C}_1} - \frac{1}{C_1}\right) \Rightarrow C_1 = \frac{\tilde{C}_1}{\tilde{C}_1 r_2 - 1} \qquad (11)$$

The same reasoning is applied to identify the real value of capacitor C_2 in case of fault of type F_8 related to C_2.

4. EXPERIMENTATION AND OBTAINED RESULTS

In order to evaluate the proposed approach, simulations were carried out for the three-cell converter using Matlab-Simulink^{TM} environment and Stateflow^{TM} toolbox. The parameters used in these simulations are:

$E = 60V, \tilde{C}_1 = \tilde{C}_2 = 40\mu F, R = 200\Omega, L = 0.1H$.

In order to highlight the efficiency of the diagnoser, the simulations take into account the set of faults defined in Table 1 for the three-cell converter.

Discrete controller commands are assured by a pulse width modulation (PWM) signal (Defoort *et al.*, 2011). Fig.7 depicts the control of three switches S_1, S_2 and S_3. When the triangular signal is below the reference signal (ref in Fig.7), the associated switch is controlled to be opened. When the triangular signal is above the reference signal, the associated switch is controlled to be closed. This sequence of control is periodic with a period of $T_{PWM} = 0.02\ s$.
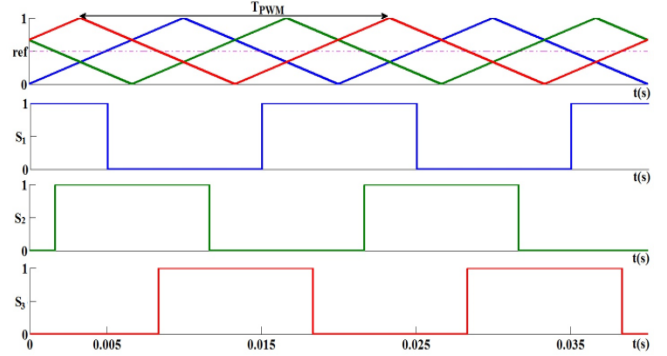

Figure 7. PWM for control of three switches S_1, S_2 and S_3.

4.1. Normal conditions scenario

Fig.8 depicts, respectively, the signals of floating voltages Vc_1 and Vc_2 and the current I. These signals correspond to the normal conditions. Moreover, one can see in Fig.8 that Vc_1 (respectively Vc_2) has a periodic signal corresponding to load and unload of capacitor C_1 (respectively C_2) around the mean value $Vc_{1ref} = \frac{E}{3} = 20V$ (respectively $Vc_{2ref} = \frac{2E}{3} = 40V$) and that the current I remains constant in the region of its reference value (0.15A).

Fig.9 shows the real and nominal dynamic evolution of Vc_1 ($\dot{V}c_1$ and $\tilde{\dot{V}}c_1$), Vc_2 ($\dot{V}c_2$ and $\tilde{\dot{V}}c_2$) and I ($\dot{I}$ and $\tilde{\dot{I}}$). We can notice that the curves representing the real and nominal dynamic evolutions are superposed. Consequently, residuals r_1, r_2 and r_3 are equal to zero in these conditions.
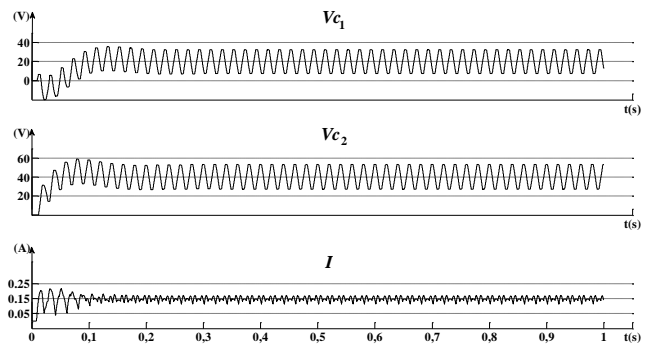

Figure 8. Real signals corresponding to Vc_1, Vc_2 and I in normal conditions .
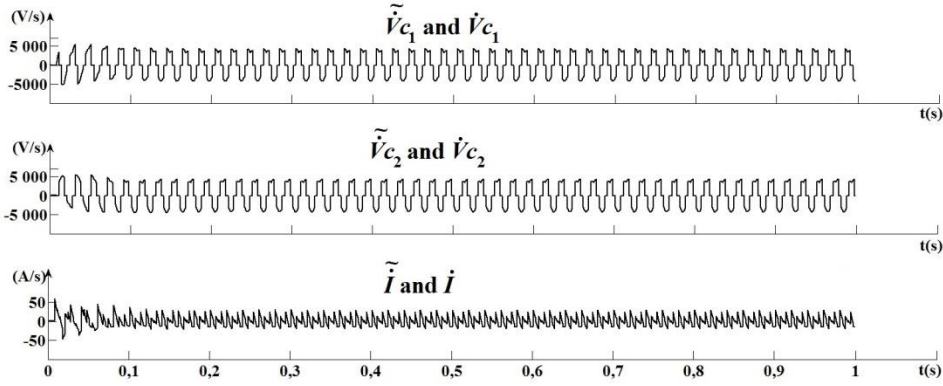
Figure 9.   Real and nominal dynamic evolution of Vc_1, Vc_2 and I in normal conditions.

4.2. Faulty conditions scenario

The test scenario is generated as follows (see Fig.10). Each fault f, belonging to one of the fault labels of Table 1, is generated starting at time t_{sf} and ending at time t_{ef}. Then, the system returns to normal operating conditions before generating a new fault for a certain time. Parametric faults of types F_7 and F_8 are simulated by changing gradualy the real values of C_1, respectively C_2, in positive or negative direction using a ramp signal. Vc_1, Vc_2 and I simulated signals including these faults are represented in Fig. 11.

One can see in Fig.11 that Vc_1 (respectively Vc_2) has lost the periodic aspects in the case of fault and that the current I has become nonconstant in the region of its reference value.

r_1, r_2, r_3 are represented in Fig.12 and Fig.13. As expected, r_1 is sensitive to the faults of types F_1, F_2, F_3, F_4 and F_7, r_2 is

sensitive to the faults of types F_3, F_4, F_5, F_6 and F_8 while r_3 is sensitive to the faults of types F_1, F_2, F_3, F_4, F_5 and F_6.

Fig.14, Fig.15, Fig.16 and Fig.17 show, respectively, local decision (SP_1) of diagnoser D_1, local decision (SP_2) of diagnoser D_2, local decision (SP_3) of diagnoser D_3 and global decision (SP).

The first local diagnoser D_1 is sensitive to faults of types F_1, F_2 and F_7 (diagnosis with certainty their ocurence), the second local diagnoser D_2 is sensitive to faults of types F_3, F_4, F_7 and F_8 while the third local diagnoser D_3 is sensitive to faults of types F_5, F_6 and F_8. We can conclude that the global decision indicates with certainty the occurrence of each of the generated faults. The diagnosis delay corresponds to the time when the system is in a discrete fault is due to residues that are silent in some discrete state.

Figure 10.   Time of apperance, injection, of faults during the simulation of three cell converter.
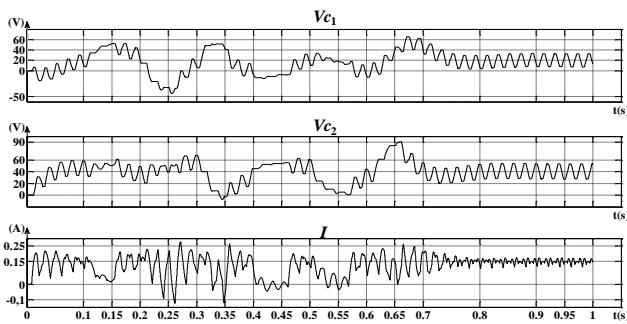
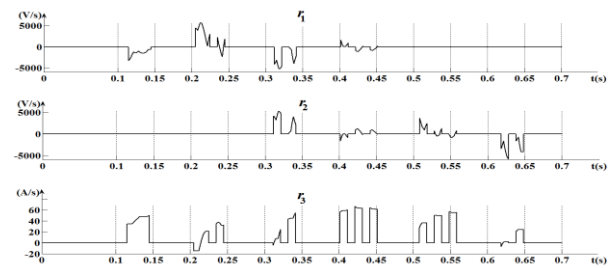Figure 11.   Real signals of Vc_1, Vc_2 and I in faulty and normal conditions.

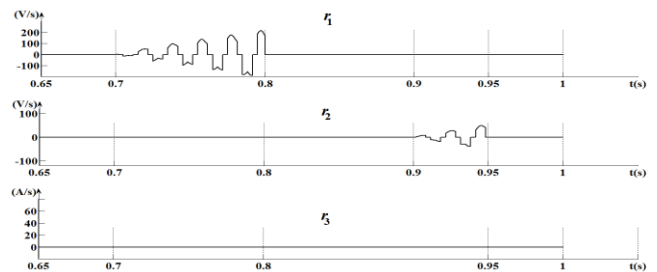Figure 12.   Residuals corresponding to generated discrete faults of Fig.10.

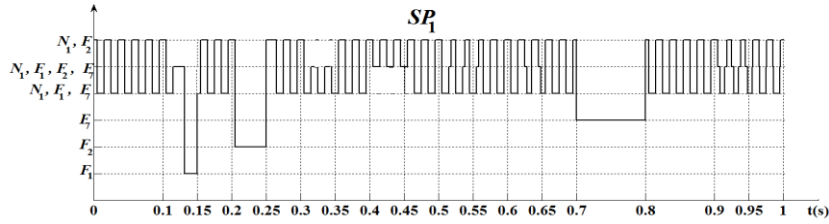Figure 13.   Residuals corresponding to generated parametric faults of Fig.10.

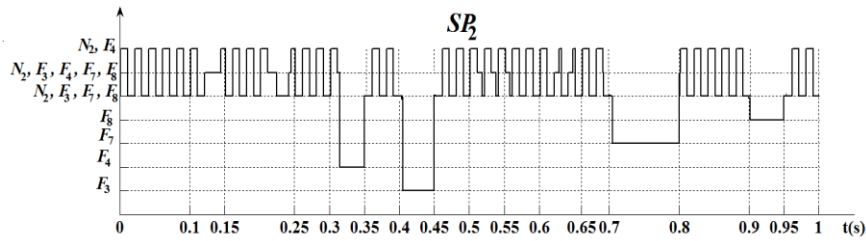Figure 14. Local decision (SP_1) of D_1.
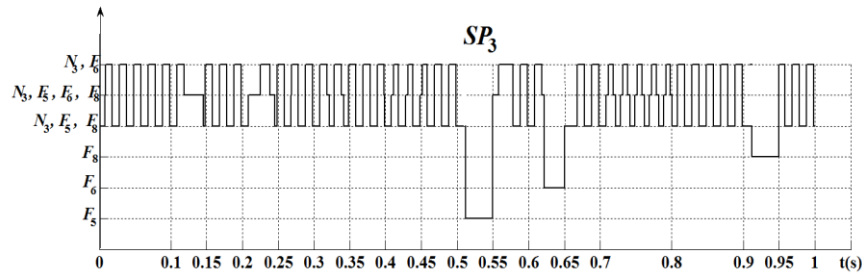

Figure 15. Local decision (SP_2) of D_2.

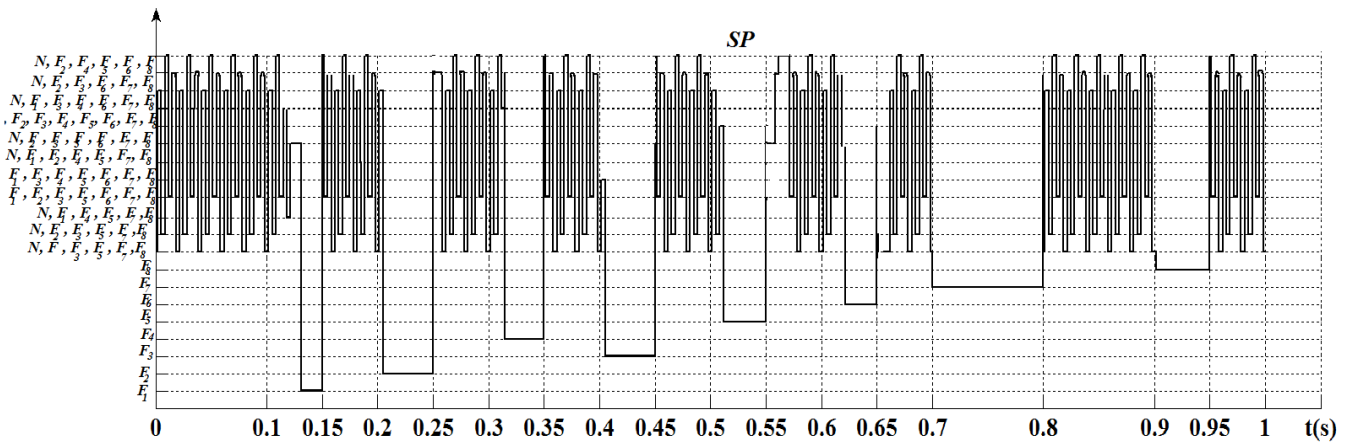Figure 16. Local decisions (SP_3) of D_3.

Figure 17. Global diagnosis decision issued by the coordinator.

4.3. Normal conditions with noises in parameters scenario

Diagnosis algorithms should be tested and evaluated on real systems with practical significance. In these systems, factors such as noise make diagnosis challenging. Therefore, there is a need to evaluate the robustness of the diagnosis algorithms for different fault and noise magnitudes.

Accurate simulation models of the system are required for this purpose. Further, it is important to execute the diagnosis algorithms on systems, where model uncertainty is always present, and complicates the diagnosis task. In order to examine the robustness of our approach, a parametric noise (see for example Fig.18), applied on parameters, is used. From an electrical point of view, the resistors are the most disturbing element in tree cell converter systems. For this

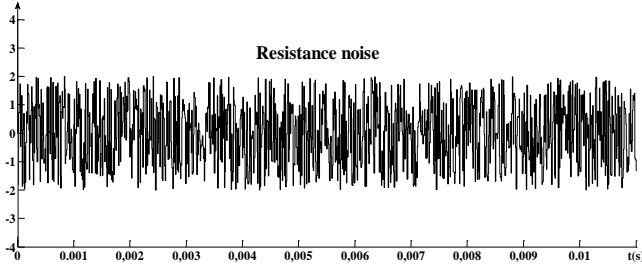reason, we simulated noise on signal resistance.

Figure 18.   Noise added to resistance R in the converter.

In order to take into account the noises in R, the residuals of (4) is written as follows:

$$\begin{cases} r_1 = \left(-\tilde{h}_q^1 \frac{1}{\tilde{C}_1} + h_q^1 \frac{1}{C_1}\right)I + \left(\tilde{h}_q^2 \frac{1}{\tilde{C}_1} - h_q^2 \frac{1}{C_1}\right)I \\ r_2 = \left(-\tilde{h}_q^2 \frac{1}{\tilde{C}_2} + h_q^2 \frac{1}{C_2}\right)I + \left(\tilde{h}_q^3 \frac{1}{\tilde{C}_2} - h_q^3 \frac{1}{C_2}\right)I \\ r_3 = \left(-\tilde{R} + R_b\right)\frac{I}{L} + \left(\tilde{h}_q^1 - h_q^1\right)\frac{Vc_1}{L} + \\ \qquad \left(\tilde{h}_q^2 - h_q^2\right)\frac{(Vc_2 - Vc_1)}{L} + \left(\tilde{h}_q^3 - h_q^3\right)\frac{(E - Vc_2)}{L} \end{cases} \quad (12)$$

Where $\tilde{R}$ is the nominal value of R without noises while R_b is the real value of R. The latter corresponds to the nominal value of R with noises.

r_1, r_2, r_3 are represented in Fig.19. As expected, r_1 and r_2 are not sensitive to this perturbation in normal conditions (R does not influence the dynamic evolution of Vc_1 and Vc_2. While r_3 is impacted by this noise. It changes between $-0.4A/s$ and $0.4A/s$.
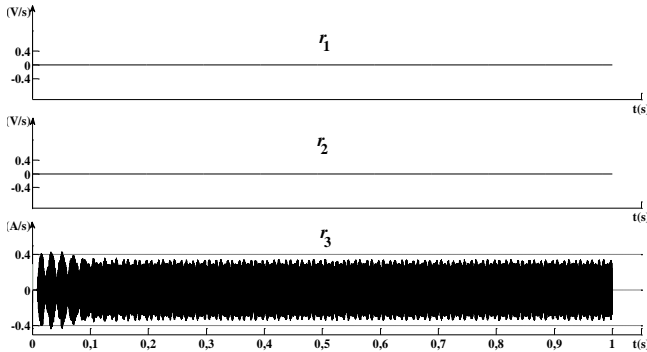

Figure 19.   Set of residuals with noise corresponding to the normal conditions.

Ideally, any non-zero residual value implies a fault, which should trigger the fault isolation system. Therefore, statistical techniques are required for reliable fault detection. The fault detection system is based on a Z-test that uses the estimated variance of the residuals and a pre-specified confidence level to establish the significance of observed nonzero residuals. To cope with noise, we compute the mean and the variance at different time points (Biswas *et*

al., 2003). The Z-test is a statistical inference test employed to establish the signification of the deviation. It requires the mean and standard deviation of the population, and the mean and size of the samples. These values are estimated using sliding windows over the residual for a variable. A small sliding window of size $W_1 = 5$ samples, is used to estimate the current mean $\mu_{r_i}(t)$ of the residual r_i related to the variable x_i:

$$\mu_{r_i}(t) = \frac{1}{W_1} \sum_{v=t-W_1+1}^{t} r_i(v) \quad (13)$$

We suppose the mean of the population is equal to zero, since the residual should be zero when the system is free of faults. We compute the variance from data history of the nominal residual signal over a window W_2 proceeding W_1 as an estimate of the true variance:

$$\mu'_{r_i}(t) = \frac{1}{W_2} \sum_{v=t-W_2-W_1+1}^{t-W_1} r_i(v) \quad (14)$$

$$\sigma_{r_i}(t) = \frac{1}{W_2} \sum_{v=t-W_2-W_1+1}^{t-W_1} \left(r_i(v) - \mu'_{r_i}(v)\right)^2 \quad (15)$$

The size of W_2 must contain enough of measurements in order to estimate correctly the residuals' mean and variance in the normal operating conditions and therefore to reduce the rate of false alarms. The size of W_1 must also be selected as a tradeoff between the delay of fault detection and the rate of false alarms. The size of W_2, respectively W_1, is chosen experimentally to be equal to 25, respectively 5, measurements.

Since the distribution of residuals mean is supposed to follow the normal distribution, a confidence level, α, is defined by determining the bound $\left[\mu_{r_i}^-, \mu_{r_i}^+\right]$ within which $\mu_{r_i}(t)$ is considered to correspond to normal operating conditions. $\left[\mu_{r_i}^-, \mu_{r_i}^+\right]$ is defined using Z-test table and the approximation σ_{r_i}:

$$\mu_{r_i}^- = \frac{z_{v_i}^- \sigma_{r_i}}{\sqrt{W_1}} \quad (16)$$

$$\mu_{r_i}^+ = \frac{z_{v_i}^+ \sigma_{r_i}}{\sqrt{W_1}} \quad (17)$$

For α equal to 0.95, $z_{v_i}^-$ and $z_{v_i}^+$ are equal to, respectively, -1.64 and 1.64.

The Z-test is employed in the following manner:

$\mu_{r_i}^- < \mu_{r_i} < \mu_{r_i}^+ \Longrightarrow$ No fault

Otherwise $\Longrightarrow$ Fault

Fig.20 depicts mean of residuals μ_{r_3} and the negative and positive thereshold of this residual. The mean and true variance of residual r_1 and r_2 are equal to zero. Thus its thereshold is also equal to zero (μ_{r_1}, $\mu_{r_1}^-$ and $\mu_{r_1}^+$,respectively, μ_{r_2}, $\mu_{r_2}^-$ and $\mu_{r_2}^+$ are superposed).
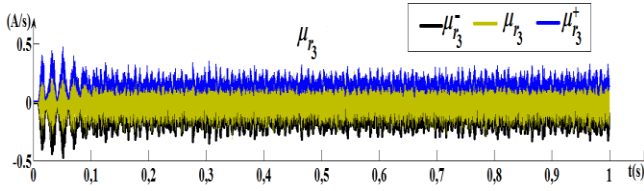
Figure 20.   Set of residuals and thersholds with noise corresponding to the normal conditions.

In case of fault, Table 4 is used to achieve a local diagnosis of D_1.

Table 4. Local fault signatures generated due to the occurrence of faults in HC_1 in case of parametric noise.

SP^1	Local signature name	Equivalent global fault signatures
F_1	Sig_1^1	$\left(\frac{-I}{C_1}+\mu_{r_1}^- < \mu_{r_1} < \frac{-I}{C_1}+\mu_{r_1}^+\right)\&\left(\mu_{r_2}^- < \mu_{r_2} < \mu_{r_2}^+\right)\&\left(\frac{Vc_1}{L}+\mu_{r_3}^- < \mu_{r_3} < \frac{Vc_1}{L}+\mu_{r_3}^+\right)$
F_2	Sig_2^1	$\left(\frac{I}{C_1}+\mu_{r_1}^- < \mu_{r_1} < \frac{I}{C_1}+\mu_{r_1}^+\right)\&\left(\mu_{r_2}^- < \mu_{r_2} < \mu_{r_2}^+\right)\&\left(\frac{-Vc_1}{L}+\mu_{r_3}^- < \mu_{r_3} < \frac{-Vc_1}{L}+\mu_{r_3}^+\right)$
F_7	Sig_{71}^1	$\left(\mu_{r_1}^- > \mu_{r_1}\right)\&\left(\mu_{r_2}^- < \mu_{r_2} < \mu_{r_2}^+\right)\&\left(\mu_{r_3}^- < \mu_{r_3} < \mu_{r_3}^+\right)$
	Sig_{72}^1	$\left(\mu_{r_1}^+ < \mu_{r_1}\right)\&\left(\mu_{r_2}^- < \mu_{r_2} < \mu_{r_2}^+\right)\&\left(\mu_{r_3}^- < \mu_{r_3} < \mu_{r_3}^+\right)$
N_1	Sig_N^1	$\left(\mu_{r_1}^- < \mu_{r_1} < \mu_{r_1}^+\right)\&\left(\mu_{r_2}^- < \mu_{r_2} < \mu_{r_2}^+\right)\&\left(\mu_{r_3}^- < \mu_{r_3} < \mu_{r_3}^+\right)$

The other diagnosers D_2 and D_3 for HC_2 and HC_3 can be constructed similarly as for D_1.

4.4. Faulty conditions with parameters perturbation

In order to evaluate the proposed approach in case of noise, another scenario of fault is generated (see Fig.21). The corresponding $\mu_{r_1}, \mu_{r_2}, \mu_{r_3}$ for this senario are represented in Fig.22. and Fig.23. In this case, noises are observed only in r_3 at normal and faulty conditions (see zoom in Fig.24). As we said before, only r_3 is impacted by noises since the noisy parameter R is included only in dynamic evolution $\dot{I}$ of I (see (1)). To overcome this problem, a threshold is defined for each residual using Z-test. These thresholds are used during the fault detection and isolation in order to avoid the false alarms as well as the fault missed detection caused by noises.
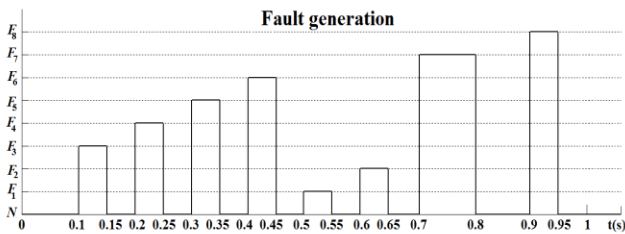

Figure 21.   Time of apperance, injection, of faults during the simulation of three cell converters with noise.
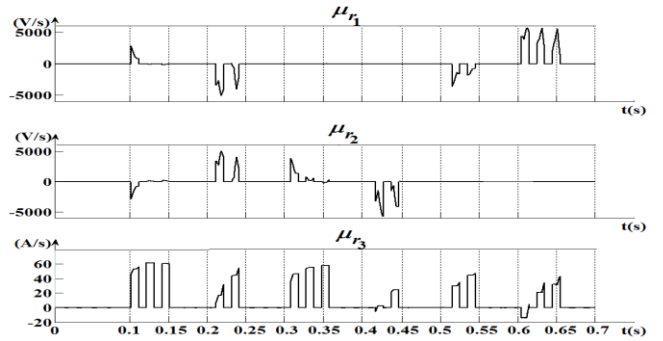

Figure 22.   Residuals corresponding to generated discrete faults of Fig.21 in case of noise.
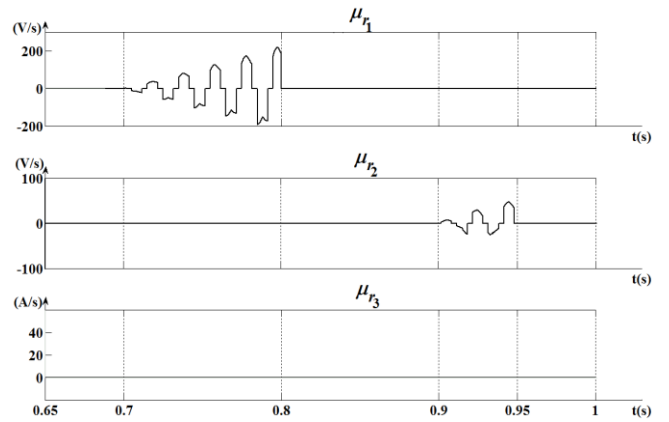

Figure 23.   Residuals corresponding to generated parametric faults of Fig.21 in case of noise.
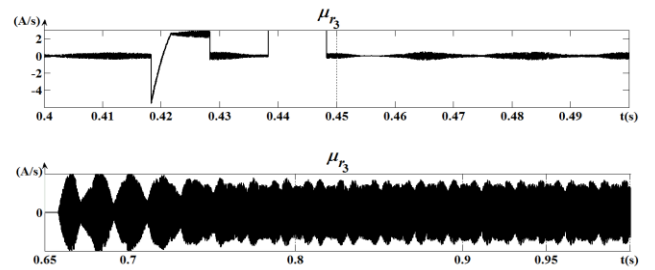

Figure 24.   Zoom of residuals signals with noise corresponding to normal and faulty conditions.

Fig.24, Fig.25, Fig.26 and Fig.27 show, respectively, local decision (SP_1) of diagnoser D_1, local decision (SP_2) of diagnoser D_2, local decision (SP_3) of diagnoser D_3 and global decision (SP). The first local diagnoser D_1 is sensitive to faults of types F_1, F_2 and F_7 (diagnosis with certainty their ocurence), the second local diagnoser D_2 is sensitive to faults of types F_3, F_4, F_7 and F_8 while the third local diagnoser D_3 is sensitive to faults of types F_5, F_6 and F_8. We can conclude that the global decision indicates with certainty the occurrence of each of the generated faults regardless of the existence of noise.
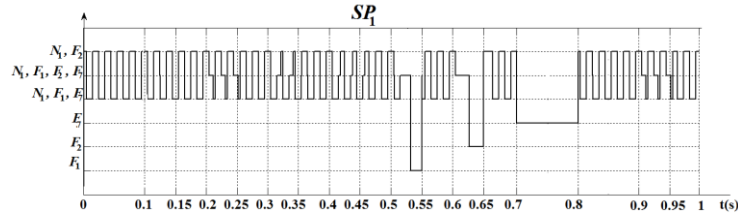
11

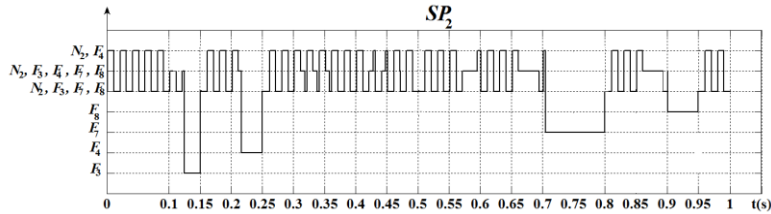Figure 25.   Local decisions (SP_1) of D_1 in case of noise.

Figure 26.   Local decisions (SP_2) of D_2 in case of noise.
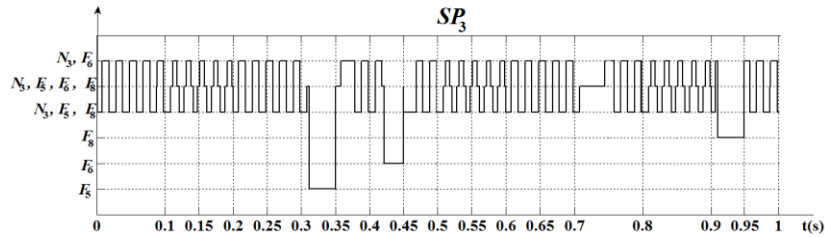

Figure 27.   Local decisions (SP_3) of D_3 in case of noise.
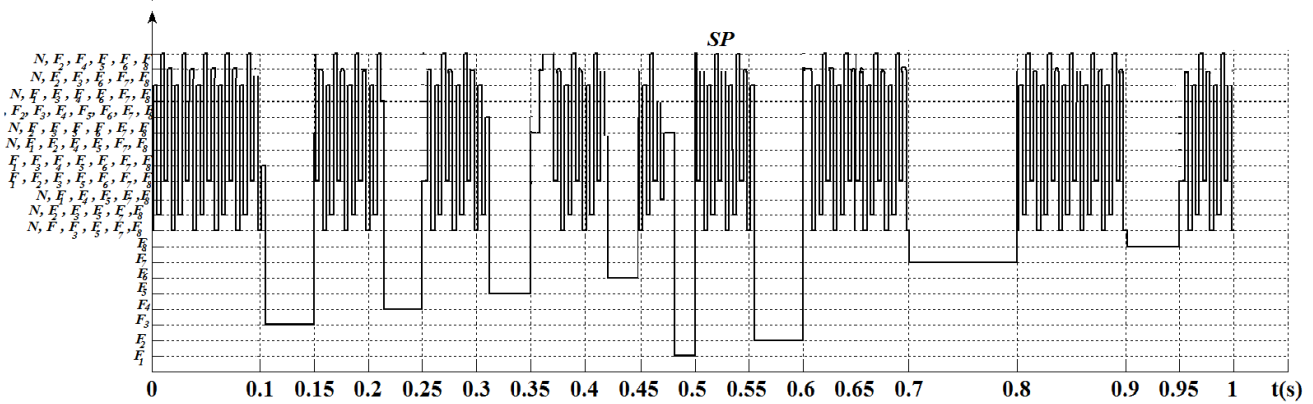

Figure 28.   Global diagnosis decision issued by the coordinator in case of noise.

5.   CONCLUSION

In this paper, a decentralized hybrid diagnosis approach for discretely controlled continuous systems is proposed. The elaboration of this approach is motivated by the capacity of the hybrid models to represent intrinsically the interactions between the continuous and the discrete dynamics of a system.

The originality of this work is the exploitation of the system modularity in order to reduce its complexity as well as the explosion in the number of its discrete states. To achieve that, the diagnosis task is accomplished by a set of local hybrid diagnosers. Each of the latter is responsible of the diagnosis of a specific part of the system. These local hybrid diagnosers are built without the use of the system global model but only local models. The decisions of the local hybrid diagnosers are merged using a coordinator in order to obtain a diagnosis performance equivalent to the one of a centralized diagnosis structure.

In the future work, this approach will be applied to a real

three-cell converter. Then, it will be developed to consider multiple and adjacent faults in a more general class of hybrid dynamic systems.

REFERENCES

Alavi M., Luo M., Wang D., and Zhang D., 2011. "Fault diagnosis for power electronic inverters: a model-based approach," in IEEE International Symposium on Diagnostics for Electric Machines, Power Electronics & Drives (SDEMPED).

Arogeti S., Wang D., and Low C. B., 2010. "Mode identification of hybrid systems in the presence of fault," Industrial Electronics, IEEE Transactions on, vol. 57, no. 4, pp. 1452–1467.

Bayoudh M., Trave-Massuyés L., and Olive X.. 2006. Hybrid systems diagnosability by abstracting faulty continuous dynamics. In Proceedings of the 17th International Workshop on Principles of Diagnosis DX'06, pp. 9–15.

Bhowal P., Sarkar D., Mukhopadhyay S., and Basu A., 2007. "Fault diagnosis in discrete time hybrid systems - a case study," Information Sciences, vol. 177, pp. 1290–1308.

Biswas S., Sarkar D., Mukhopadhyay S., and Patra A., 2006. "Diagnosability analysis of real time hybrid systems", Industrial Technology. IEEE International Conference on, pp. 104–109.

Biswas G., Simon G., Mahadevan N., Narasimhan S., Ramirez J., and Karsai G., 2003. "A robust method for hybrid diagnosis of complex systems", In Proceedings of the 5th Symposium on Fault Detection, Supervision and Safety for Technical Processes, pp.1125-1131.

Cocquempot V., El Mezyani T., and Staroswiecki M., 2004."Fault detection and isolation for hybrid systems using structured parity residuals," in Proceedings of the 5th IEEE/IFACASCC: Control Conference, Asian.

Daigle M., Koutsoukos X., and Biswas G., 2010. "An event-based approach to integrated parametric and discrete fault diagnosis in hybrid systems," Transactions of the Institute of Measurement and Control, vol. 32, pp. 487–510.

Derbel H., Alla H., Hadj-Alouane N. and Yeddes M., 2009. "Online diagnosis of systems with rectangular hybrid automata models," in Proceedings of the 13th IFAC Symposium on Information Control Problems in Manufacturing.

Defoort M., Djemai M., Floquet T., and Perruquetti W., 2011. "Robust finite time observer design for multicellular converters," International Journal of Systems Science, vol. 42, pp. 1859–1868.

Louajri H., Sayed-Mouchaweh M., and Labarre C., 2013. "Diagnoser with hybrid structure for fault diagnosis of a class of hybrid dynamic systems," Chemical Engineering Transactions, vol. 33, pp. 85–90.

Kamel T., Diduch C., Bilestkiy Y., and Chang L., 2012. "Fault diagnoses for the dc filters of power electronic converters," in Energy Conversion Congress and Exposition (ECCE), IEEE.

Rahiminejad M., Diduch C., Stevenson M., and Chang L., 2012. "Open circuit fault diagnosis in 3-phase uncontrolled rectifiers," in Power Electronics for Distributed Generation Systems (PEDG), 3rd IEEE International.

Schild A. and Lunze J., 2008. "Switching surface design for periodically operated discretely controlled continuous systems," in Hybrid Systems: Computation and Control.

Shahbazi M., Jamshidpour E., Poure P., Saadate S., and Zolghadri M., 2013. "Open- and short-circuit switch fault diagnosis for nonisolated dc-dc converters using field programmable gate array," Industrial Electronics, IEEE Transactions on, vol. 60, no. 9, pp. 4136–4146.

Trigeassou J.-C., 2011. " Diagnostic des machines électriques ". Lavoisier.

Uzunova M., Ould-Bouamama B., and Djemai M., 2012. "Hybrid bond graph diagnostic and localisation-signal signature study of three-cell converter," in Mediterranean Conference on Control & Automation (MED), Barcelona, Spain.

Zaytoon J., 2001. " Systèmes dynamiques hybrides". Hermès science publications.

BIOGRAPHIES

Hanane Louajri received her Master degree in Complex Systems Engineering section Automatic and Embedded data Processing from the University of Nancy in 2011. She received his engineering degree in Automatic and Computer Engineering from the High Engineering School "Ecole Marocaine des Sciences de l'Ingénieur" in 2011. She is currently PhD student in the High National Engineering School of Mines "Ecole Nationale Supérieure des Mines de Douai" at the Department of Automatic Control and Computer Science. Her research interests are diagnosis of hybrid dynamic systems.

Moamar Sayed-Mouchaweh received his Master degree from the University of Technology of Compiegne-France in 1999. Then, he received his PhD degree from the University of Reims-France in December 2002. He was nominated as Associated Professor in Computer Science, Control and Signal processing at the University of Reims-France in the Research center in Sciences and Technology of the Information and the Communication (CReSTIC). In December 2008, he obtained the Habilitation to Direct Researches (HDR) in Computer science, Control and Signal processing. Since September 2011, he is working as a Full Professor in the High National Engineering School of Mines "Ecole Nationale Supérieure des Mines de Douai" at the Department of Automatic Control and Computer Science (Informatique & Automatique IA).